Jurgita Domskienė,
Eugenija Strazdienė

Kaunas University of Technology
Faculty of Design and Technology
Studentų 56, LT-51424 Kaunas, Lithuania
E-mail: jurgita.domskiene@ktu.lt
eugenija.strazdiene@ktu.lt

Investigation of Fabric Shear Behaviour

Abstract
The shear behaviour of fabrics and the phenomenon of buckling is analysed during the uniaxial tension of a bias cut specimen. The image analysis method is proposed to define critical shearing conditions and to analyse the deformation processes of bias-stretched fabric. The critical tension load, critical elongation and critical shear angle are defined on the basis of a grey-scale value I variation in the images of the fabric specimen. It is found that the dispersal of a grey-scale value CV can be used to estimate the surface waviness of stretched fabric. It is shown that a simple uniaxial tension experiment supplemented by image analysis can be used not only to define the shear parameters of a fabric but also to explain fabric behaviour in greater depth due to analysis of the buckling phenomenon.

Key words: *fabric, shear angle, uniaxial tension, buckling, image analysis.*

Introduction

The shearing behaviour of a fabric determines its performance properties when subjected to a wide variety of complex deformations in use. The ability of a fabric to be deformed by shearing distinguishes it from other thin sheet materials such as paper or plastic films. This property enables fabric to undergo complex deformations and to conform to the shape of the body. Shearing influences draping, flexibility and also the handle of woven fabric. Shear properties are important not only for fabrics but for textile composites as well.

There is a considerable amount of literature analysing the shear behaviour of fabrics and aimed at developing prototype tests and apparatus for the determination of shear properties [1-14]. The buckling of fabrics during shearing has been a major problem in designing ideal testing equipment. Sheet-form materials whose flexural and tensile rigidity are very low require elaborate devices to measure shear and buckling. Three major methods are known and widely used to determine fabric shear properties (Figure 1), but it must be noted that in nearly all these methods, the phenomena of shear locking and specimen buckling are ignored.

Shear angle is one of the main criteria for characterising the formability of fabrics. As the fabric is fitted onto a spatial surface, shearing occurs increasingly until the critical shearing angle is reached. When this angle exceeds a strict value, the specimen starts to buckle, i.e. wrinkling is observed. The major problem is to specify the onset of specimen buckling. Frequently changes in the deformed specimen's surface are observed visually, but some studies have been done to evaluate fabric buckling objectively. The critical buckling load was calculated using the criterion based on the cantilever beam theory [3,8], but in other studies [7,9] it was found that the onset of buckling does not appear to agree with this criterion. There are some numerical methods to calculate fabric buckling in the KES-F shear test [16] and the uniaxial tension of the bias-cut specimen [17,18] but to implement these methods more in-depth studies are required. So the onset of specimen wrinkling, i.e. the critical shear angle, is often not recorded, and other criteria are used for fabric shear evaluation: shear rigidity and shear stresses at different constant shear angle.

The aim of this investigation was to establish a simplified method for critical shear angle estimation during the uniaxial tension of a bias-cut fabric specimen. The surface wrinkling of the deformed specimen is observed by image analysis. New quantitative criteria are defined to specify the onset of surface buckling and to evaluate the level of specimen wrinkling.

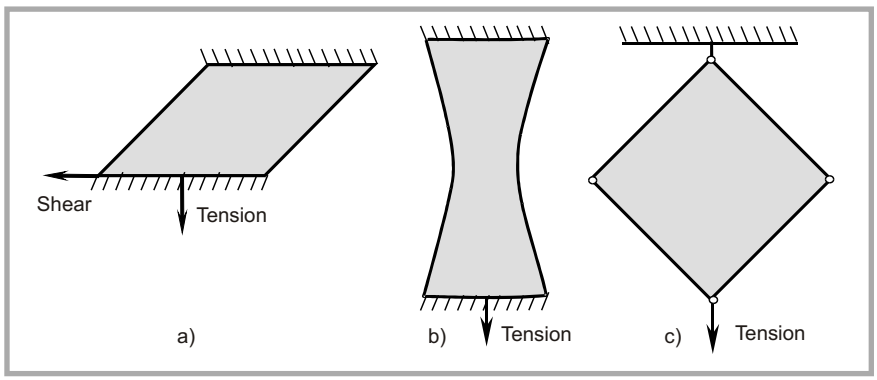

Figure 1. *Principal of shear tests: a - KES-F [13-14], b - FAST [1], c - picture frame [17].*

Background

W.F. Kilby [19] has shown that shear rigidity can be calculated from the tensile properties of a fabric in bias (45°) direction based on the interrelations of the in-plane properties of a plate. The uniaxial tension of a bias-cut fabric specimen is relatively simple and may be carried out on any extensometer. This method of fabric properties investigation is therefore the most appropriate for industrial use. However, when this test is applied to fabric, shearing is non-uniform throughout the specimen due to the distortion of width uniformity. Three basic zones with different modes of deformation can be distinguished [20] (Figure 2). Zones I form near the clamps at each end of the specimen. There is no significant deformation in this zone. Zones II consist of four identical triangular regions neighbouring zone I. There are some changes in thread angle in this zone, but not so significant as in zone III. Zone III is located between zones I and II. This zone is free from the constrained ends boundary effects, and most of the deformation in the fabric specimen occurs here. The main mode of deformation in zone III is shear, with pure shearing in the middle of the specimen [20].

When tension load is applied to the bias-cut (45° angle to the warp thread direction) woven specimen, the dependence between the load and specimen elongation can be schematically described as a

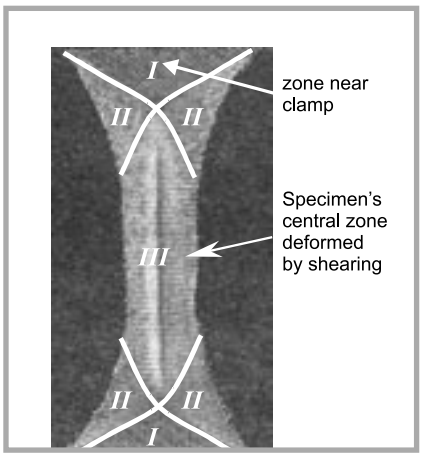

Figure 2. *Zones formed in the bias tension of a fabric.*

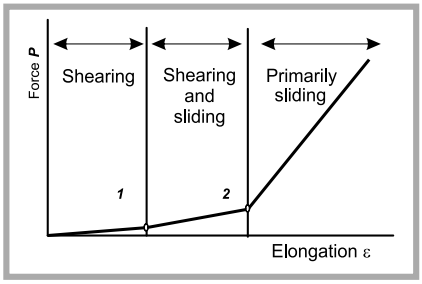

Figure 3. *Schematic presentation of dependence between tension load P and elongation ε of bias-cut specimen.*

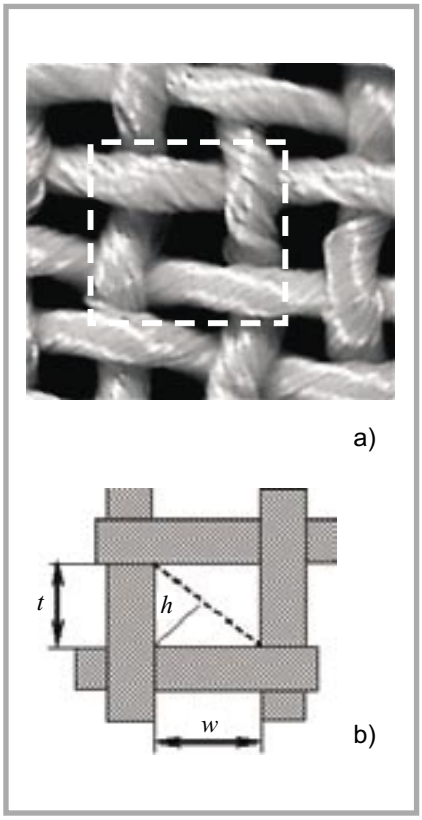

Figure 4. *The views of plain weave fabric (a) and one of its basic cells , as considered in the microstructural analysis of shear deformation (b).*

tri-linear relationship [20]. The first part of the P-ε curve (Figure 3) represents the initial shearing when the angle between threads changes in the central part (zone III) of the stretched fabric specimen (Figure 2). At the first point when the critical shearing angle is reached (point 1 in Figure 3), the threads in the specimen's central part are packed tightly. The increase in tension causes a lateral compression of the threads, so the buckling wave is formed. The stiffness of fabric increases, and the force required to deform the specimendoes so as well. The second part of the curve P-ε represents deformations from thread shearing due to thread sliding; thus the changes in the buckling wave parameters are observed. Point 2 of the tension curve P-ε indicates the beginning of the third part of the curve, when the predominant mode of deformation becomes thread sliding, because the locking shearing angle has been reached and the threads cannot shear any more. The lateral compression of threads decreases and the fabric surface waviness declines gradually.

The buckling of a specimen during shearing is associated with the level of compressive stresses, thickness and stiffness of a fabric and its structure [21]. In plain weave fabric, the critical shear angle is associated with the disappearance of macropores between threads. Figure 4 represents the basic cell of plane weave. The critical shear angle γ'_{cr} can be calculated as follows: [21]:

$$\gamma'_{cr} = \pi/2 - arc\sin(h/w) - arc\sin(h/t) \quad (1)$$

where w and t are dimensions of the original macropore, and h is height (see Figure 4b).

Experimental

The image analysis method was used to define the different parameters of fabric behaviour under uniaxial tension (Figure 5). The bias-cut specimen 2 was fixed in a standard tensile testing machine. The images of stretched specimen 2 were captured by a digital camera 1 at each 10% step up to 50% of the longitudinal specimen deformation (Figure 6) in order to investigate not only the shearing processes of the fabric but also the buckling phenomenon as well. The ruler 4, able to measure to the nearest 1 mm, was used for image calibration.

The method for evaluating fabric surface waviness during tension has been

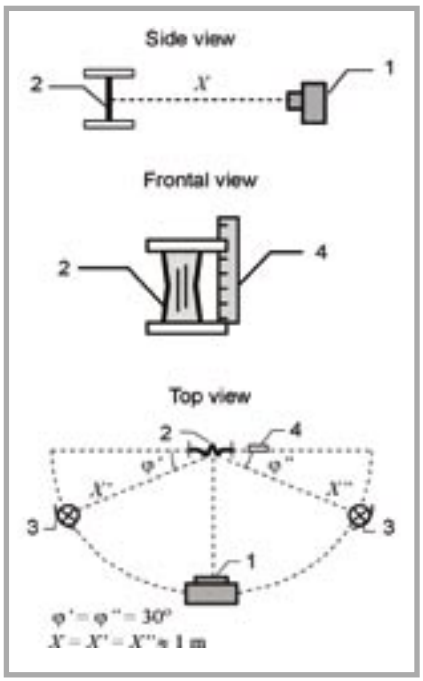

Figure 5. *Test arrangement for stretched specimen capturing: 1 - digital camera, 2 - specimen, 3 - lighting sources, 4 - ruler.*

presented in earlier studies [22,23]. The variation of the grey-scale value I in the deformed specimen image was used to estimate the surface waviness of the stretched fabric. The deformed specimen, as captured by the digital camera, was stored as a grey-scale image of 256 levels. By applying additional filters of image processing, the quality of the image was improved and noise was reduced, preparing the image for analysis. Surface waviness analysis using models of known shape [22,23] showed that the buckling of a fabric can be evaluated by the dispersal of the grey-scale level CV. The profile curve and grey-scale level histogram of the central part of the stretched specimen were used to calculate this parameter:

$$CV = \frac{s}{\bar{I}} \quad (2)$$

where s is the standard deviation of grey-scale value I defined from the histogram at the horizontal middle line, $\bar{I}$ is the average of the grey-scale value in the analysed line, expressed as:

$$\bar{I} = \frac{\sum_{i=1}^{e} I_i}{e} \quad (4)$$

where I_i is the i grey-scale value, and e is the total number of pixels in the analysed line.

While analysing the behaviour of bias fabric under tension, it was important

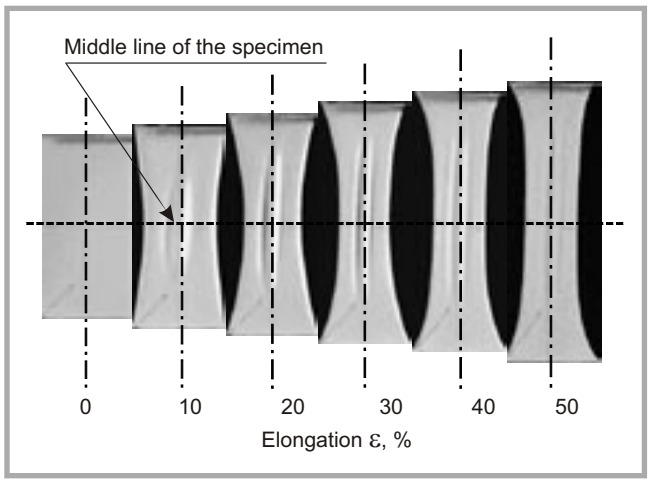

Figure 6. *Digital images of stretched specimen after filtering (elongation increases from 0% to 50%).*

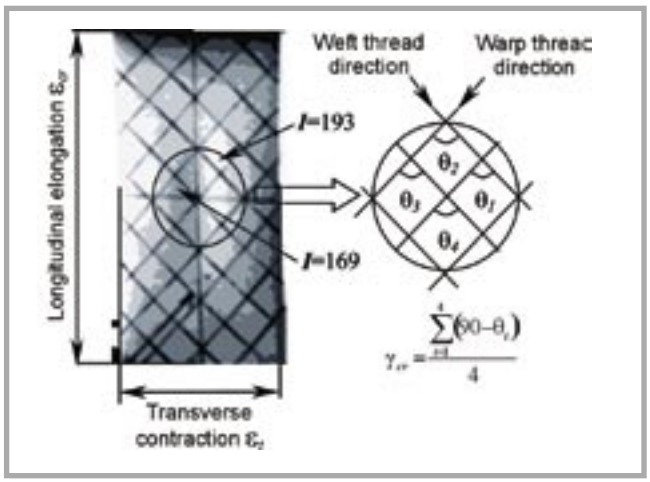

Figure 7. *The variation of the grey scale value I in digital image of the stretched specimen and the principle scheme of shear angle calculation.*

to define precisely the moment when the critical shear angle is reached in the deformed specimen, i.e. the moment when the surface of specimen started to wrinkle. The same image analysis system was adjusted to investigate the critical buckling conditions of a stretched fabric. The capturing was performed at different directions of light source. It was decided that the light at 90° angle in respect to the stretched specimen surface enabled even the negligible surface waviness of the specimen to be fixed. The buckling of bias fabric was revealed under very low stress, and so the test was performed using FAST-3 equipment. The images of the deformed specimen were captured by increasing the tension load by steps of 20 g (≈ 3.9 N/m) up to the value of 1000 g (≈ 100 N/m). After the processing of digital images by special filters and functions, the starting point of buckling wave formation was considered to be the moment when the variation of the grey-scale value I was recorded (Figure 7). This is the start point of the specimen surface wrinkling. Testing conditions corresponding to that point (tensile force P_{cr}, elongation ε_{cr}, shear angle γ_{cr}) were registered.

In order to determine the shear angle, a net of perpendicular lines 10×10 mm (accuracy ±1 mm) in weft and warp directions was plotted on the specimen surface (Figure 7). Shear angle was calculated as the average of four adjacent shear angles at the centre part of the specimen.

For the investigations, three types of fabrics were chosen: traditional (marked A), coated (marked C) and laminated (marked L). Their main characteristics are presented in Table 1. All the chosen fabrics were of the same plain weave, but differed in properties.

Results and Discussion

The behaviour in bias tension of the chosen fabrics did not differ markedly, especially in the first part of curve P-ε (Figure 8). However, their shearing and buckling analyses did show some peculiarities.

When the tension load is increased, the shear angle in a centre part of bias cut fabric increases also. The exponential dependence was determined between the tension load P and shear angle γ (Figure 9, Table 2). For fabrics, the sharp increase of tension curve slope angle was observed when the shear angle in specimens centre reached 40-45°. These results of shear angle variation in uniaxial tension agree with the results of similar research presented in paper [10]. The different behaviour of fabrics in both bias tension and shearing depends on the fabric's structure and stiffness properties. It was noted that the shear angle of tested fabrics reached the value of 45° under 25-35% of elongation (Figure 10). Only for coated fabric C10 were different shear angle variation and lower values observed.

Table 2. *Coefficients a, b of exponential function $P=ae^{b\gamma}$ and determination coefficient R^2.*

Fabric code	a	b	R^2
A3	14.78	0.98	0.92
A4	4.26	0.13	0.95
C10	1.91	0.16	0.89
C21	276.78	0.02	0.99
L19	2.06	0.17	0.96
L20	71.37	0.08	0.97

The different behaviour of coated fabrics in uniaxial bias tension was also observed, when the buckling phenomenon of stretched specimen surface was analysed. The waviness of specimens was examined on the basis of image analysis and evaluated by grey-scale disperse CV (Figure 11). The results of these investigations have shown that the waviness of coated fabrics surface was up to 5 times higher than those obtained for classical and laminated woven fabrics.

For better understanding of fabric shear processes, the critical moment when the specimen starts to buckle is important. When applying image analysis, the critical shearing angle γ_{cr} as well as the

Table 1. *The main characteristics of investigated fabrics (PU - polyurethane, PTFE - polytetrafluorethylene).*

Properties	Fabric code					
	A3	A4	C10	C21	L-19	L20
Surface density, g/m²	190	140	190	95	210	225
Setting, cm⁻¹ warp direction weft direction	19 18	36 26	17 17	40 33	29 16	21 20
Linear density, tex warp direction weft direction	52 52	20 20	36 36	8 5	42 44	44 41
Content	100% flax	100% cotton	100% PES, coated PU	100% PA coated PU	100% PES laminated PTFE	100% PES laminated PTFE

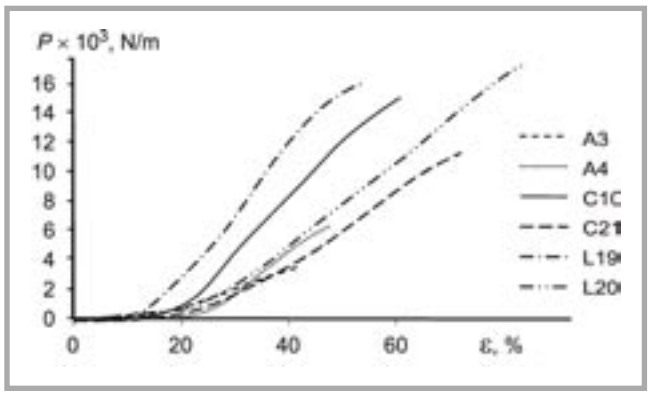

Figure 8. *Tension curves P-ε of bias cut samples.*

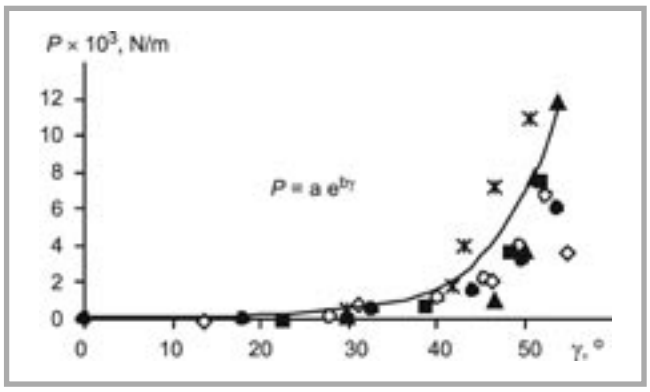

Figure 9. *The dependencies between shear angle γ and tension load P.*

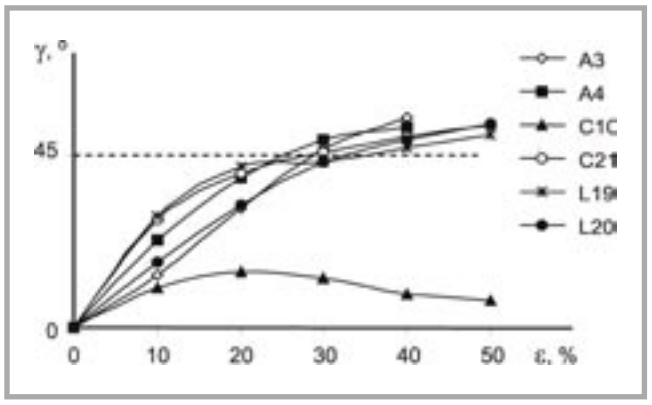

Figure 10. *The dependencies between elongation ε and shear angle γ.*

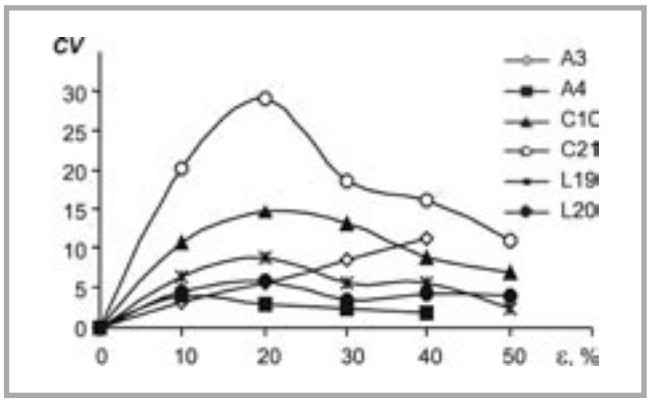

Figure 11. *The dependencies between grey-scale dispersal CV and specimen elongation ε.*

critical load P_{cr} and critical elongation ε_{cr} were defined during the uniaxial tension of the bias-cut fabric (Table 3 page 30). In the case of coated fabrics, all the spaces between the threads are filled with polymer material that firmly ties warp and weft thread systems. Thus the movement of the threads at the point of their interlacing is significantly restricted. The shearing resistance of tested coated woven fabrics C10 and C21 is high, so the critical shearing angle for this is reached at low elongation (ε_{cr}=0.6-2.8%). The method used in this research was not sufficiently sensitive to determine the real critical shear angle, so for fabric C21, γ_{cr}=0° (accuracy ±1°). The movement of the threads in the case of laminated fabrics L19 and L20 is not so highly restricted because the film is joined with the fabric only at certain points. Thus the critical shear angle of these fabrics is reached at the higher values of elongation (ε_{cr}=5.1-13.4%), and the behaviour of laminated fabrics is close to the classical woven fabrics A3 and A4.

As was mentioned earlier, the critical shear angle depends on the parameters of fabric structure. The images of fabric structure as enlarged under a microscope were used to determine the parameters w, t and h of the hole between the fabric threads (Figure 4b). Then the critical shear angle γ'_{cr} was calculated (eq. 1). A linear relationship was found between the values of shear angle defined by image analysis γ_{cr} and calculated γ'_{cr} ;in other words, the uniaxial tension of bias fabric can be used not only for shear rigidity evaluation but also to estimate the critical shear angle using the simple image analysis method. Critical shearing conditions determined at low stress provided new information concerning fabric behaviour and formability.

The comparative analysis between the tension curve, the shear angle variation and the dynamics of bucking wave variation. as well as the critical buckling conditions of the bias-cut fabric specimen, has provided that the deformational behaviour of the bias fabric under uniaxial tension can be explained more deeply by surface waviness due to the buckling phenomenon analysis [23,24].

The critical shear angle is reached at a low longitudinal deformation of the specimen. It was determined that the buckling of the specimen starts (point CV_0) before the moment when the stiffness of the specimen starts to increase; that is, the critical shearing angle γ_{cr} is reached in front of point 1 (Figure 12). The changes of the parameter CV allow us to specify when the maximum of the specimen's surface waviness is reached (point CV_{max}), i.e. when the threads are packed most closely but are still not sliding. This happens between points 1 and 3. However, in the same zone of tension curve between points 3 and 2, a decrease in surface waviness is observed. In other words, the height of

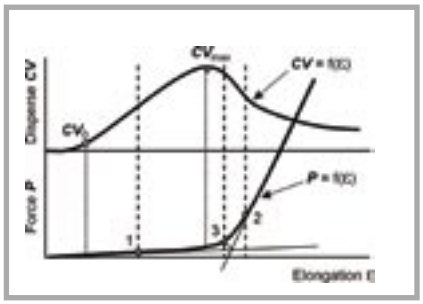

Figure 12. *Typical dependencies between tensions curve P-ε and dispersal of grey-scale CV variation during tension.*

Table 3. *Critical shearing conditions of bias stretched fabric specimens.*

Fabric code	A3	A4	C10	C21	L19	L20
Critical load P_{cr}, N/m	196.2	15.7	43.2	7.8	78.4	176.4
Critical elongation $\varepsilon_{cr,\%}$	14.2	4.6	2.8	0.6	5.1	13.4
Critical shear angle γ_{cr} ,°	33	9	5	0	7	18

the buckling wave decreases because the threads sliding appear. So, point 3 in the tension curve characterises the moment when the thread system starts to slide and the changes of shear angle become less significant.

Using more a precise specimen surface waviness and shearing angle measurement method (by analysing parameters γ and CV continually in all tensile processes with higher precision), it is possible to specify the exact moment when the thread system starts to experience the sliding phenomenon and the changes of the shear angle become negligible, i.e. when the shear 'locking angle' is reached and further tension has no influence on the thread angle changes.

Conclusions

The bias extension test is simple in essence, easy to implement and appropriate for a large range of fabrics, so it appears to be the most appropriate method for characterising fabric behaviour in shear. The proposed image analysis system can be used to defined the critical shear angle of a fabric not only in uniaxial tension but also in other shear test methods. The analysis of the tested fabrics' tensile curve, the variation of shear angle and buckling wave have showed that fabric post-buckling is associated with fabric behaviour in the tension and properties of a specimen. Further studies are under way to establish the dependencies between fabric structure, mechanical properties and buckling during uniaxial tension.

References

1. *Fabric Assurance by Simple Testing, CSIRO Division of Wool Technology. - Geelong, Australia, 1997, p. 42.*
2. *Lindberg J., Behre B., Dahlberg B. Mechanical Properties of Textile Fabrics, Part III: Shearing and Buckling of Various Commercial Fabrics, Textile Research Journal, 31(2), 1961, pp. 99-122.*
3. *Behre B. Mechanical Properties of Textile Fabrics, Part I: Shearing, Textile Research Journal, 31(2), 1961, pp. 87-93.*
4. *Grosberg P., Park B.J. The Mechanical Properties of Woven Fabrics. Part V: The Initial Modulus and the Frictional Restraint in Shearing of Plain Weave Fabrics, Textile Research Journal 36(5) 1966, pp. 420-431.*
5. *Kilby W.F. Planar Stress-Strain Relationships in Woven and Fabrics, Journal of Textile Institute, 54, 1963, pp. T9-T27.*
6. *Lindberg J., Waesterberg L., Svenson R. Wool Fabrics as Garment Construction Materials, Journal of Textile Institute, 51, 1960, pp. T1475-T1493.*
7. *Spivak, S.M. The Behaviour of Fabrics in Shear, Part I: Instrumental Method and The Effect of Test Conditions, Textile Research Journal, 36(12) 1966, pp. 1056-1063.*
8. *Cusick, G.E. The Resistance of Fabric to Shearing Forces: A Study of the Method due to Morner and Eeg-Olofsson, Journal of Textile Institute, 52(9) 1961, pp. T395-T406.*
9. *Treloar L., R., G. The Effect of the Test-Piece Dimensions on the Behaviour of Fabrics in Shear, Journal of Textile Institute, 56(10) 1965, p. T583.*
10. *Mohammed U., Lekakou C., Dong L., Bader M.G. Shear Deformation and Micromechanics of Woven Fabrics Composites: Part A 31, 2000, pp. 299-308.*
11. *Buckenham P. Bias-extension Measurements on Woven Fabrics, Journal of Textile Institute, Part I 88(1) 1997, pp. 33-40.*
12. *Page J., Wang J. Prediction of Shear Force and an Analysis of Yarn Slippage for a Plain-Weave Carbon Fabric in a Bias Extension State Composite Science and Technology 60, 2000, pp. 977-986.*
13. *Hu J., L., Zhang Y., T. The KES Shear Test for Fabrics, Textile Research Journal, 67(9) 1997, pp.654-664.*
14. *Harlock S.C. Fabric Objective Measurement: 2. Principles of Measurement Textile Asia November 1989, pp. 66-69.*
15. *Bassett R.J., Postle R. Experimental Methods for Measuring Fabric Mechanical Properties: A Review and Analysis, Textile Research Journal, 69(11) 1999, pp. 866-875.*
16. *Zhang Y. T., Xu J. F. Buckling Analysis of Woven Fabric under Simple Shear Along Arbitrary Directions, Textile Research Journal 72(2) 2002, pp.147-152.*
17. *Zhang Y.T., Fu Y.B. A Micromechanical Model of Woven Fabric and its Application to the Analysis of Buckling under Uniaxial Tension. Part 1: The Micromechanical Model International Journal of Engineering Science 38 2000, pp. 1895-1906.*
18. *Zhang Y.T., Fu Y.B. A Micromechanical Model of Woven Fabric and its Application to the Analysis of Buckling under Uniaxial Tension. Part 2: Buckling Analysis International Journal of Engineering Science 39 2001, pp. 1-13.*
19. *Kilby, W.F. Planar Stress-Strain Relationships in Woven and Fabrics, Journal of Textile Institute, 54, 1963, pp. T9-27.*
20. *Sidhu, R.M.J.S., Averill, R.C., Riaz, M., Pourboghrat, F. Finite Element Analysis of Textile Composite Preform Stamping Composite Structures 52 2001, pp. 483-497.*
21. *Mohammed U., Lekakou C., Dong L., Bader M.G. Shear Deformation and Micromechanics of Woven Fabrics Composites: Part A 31 2000, pp. 299-308*
22. *Domskiene, J., Starzdiene, E., Dapkuniene, K. The Evaluation of Technical Textiles Shape Stability by Image Analysis Material Science 8(3), 2002, pp. 304-309.*
23. *Domskiene, J. Investigation and Evaluation of Textile Materials Buckling. Doctoral dissertation. Kaunas University of Technology, 2004, p. 112.*
24. *J. Domskiene, E. Strazdiene, Shearing Behaviour of Technical Textiles. Material Science. ISSN 1392-1320. 2002, No.4, p. 489.*

Received 30.07.2004 Reviewed 19.01.2005

CORRECTION

In issue No 1(43) 2005, vol.13, in the paper of Teresa Mikołajczyk and Maciej Boguń entitled "Effect of Ceramic Nanoparticles on the Rheological Properties of Spinning Solutions of Polyacrylonitrile in Dimethylformamide" a error appeared on page 29 in Table 2. An incorrect storage time of "48 h" was given by mistake in the caption of the last columns. The storage time after which the parameters "n" and "K" were determined was in reality 168 hours.

The authors apologise to all readers and the editors for this error.

Authors